Complexity Project: The Oslo Model

Yaojia Huang
CID: 01213992
Word Count: 2471

February 18, 2019

Abstract

In this project, a computer simulation of a 1D Oslo model was constructed to investigate the nature of self-organised criticality. The result shows that the model displays scale invariance at the steady state. As the system size L goes to ∞, the height of the model converges to $(1.733 \pm 0.03)L$, and the distribution of avalanche sizes s converges to a power-law decay $\propto s^{(-1.557 \pm 0.003)}$. In a finite system, the avalanche-size distribution forms a "bump" at $s_c \propto L^{(2.245 \pm 0.002)}$ and decays rapidly thereafter. The error of the discovered relations is large in small systems because of the existence of corrections to scaling.

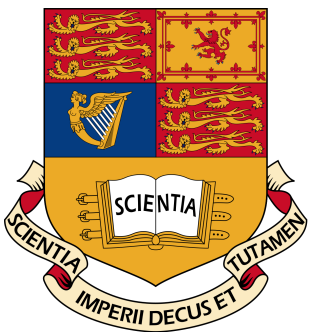

Imperial College of Science, Technology and Medicine
Department of Physics

1 Introduction

Self-organised criticality (SOC), introduced by Bak, Tang and Wiensenfeld in 1987, is a characteristic of some certain complex systems in which individual components interact locally with each other. Systems that have SOC, such as earthquakes and avalanches, can drive themselves from transient states to the steady state and display invariance at a global scale without fine-tuning at the initial stage [1].

The nature of SOC can be demonstrated by the Oslo model, which is a simulation of a slowly driven rice pile. The dynamics of the model is: (1). *Drive:* add one grain to the rice pile; (2). *Relaxation:* if the slope of any site exceeds its threshold slope, the grain on the top of that site topples, and the threshold slope of the site is reset; (3). *Iteration:* repeat the whole process [2]. The size of the avalanche triggered in one iteration is defined as the number of topplings. The Oslo model will gradually organise itself and display scale invariance if the system size is sufficiently large.

The aim of this project is to explore the scale invariance underlying the height of the Oslo model and the frequency of avalanches with different sizes.

2 Implementation of the Oslo Model

2.1 Algorithm

In a 1D Oslo model of size L, the sites are labelled from left to right in an ascending numerical order if new grains are added to the system at the leftmost site. The number of grains at site i is denoted as h_i, and the slope z_i is determined by $h_i - h_{i+1}$. The height of the model is defined as h_1. An example of an Oslo model is shown in Fig 1.

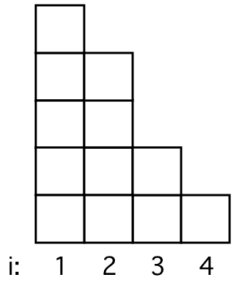

Figure 1: A typical 1D Oslo model with $L = 4$. The 1^{st} site is the place to which new grains are added.

Each site i is assigned a threshold slope $z_i^{th} \in \{1, 2\}$ and the probability of getting $z_i^{th} = 1$ is p. The dynamics of the model can be achieved via the following algorithm (based on the algorithm from [2]):

1. Create an empty system with size L and initialise z_i^{th} for all $i \in \{1, 2, ..., L\}$ according to a self-determined probability p.

2. Add one grain at the 1^{st} site:

$$z_1 \leftarrow z_1 + 1$$

3. For i from 1 to L:

If $z_i > z_i^{th}$:

$$j \leftarrow i:$$
$$z_j \leftarrow z_j - 1$$
$$z_{j-1} \leftarrow z_{j-1} + 1, \text{ (if } i \neq 1)$$

Else:

Go to the next loop

While $z_j \geq z_j^{th}$ and $j \leq L$:

Relax: $z_j^{th} = \text{Rand}(1, 2)$, (according to probability p)

$$j \leftarrow j + 1$$

If $j \neq L + 1$:

$$z_j \leftarrow z_j + 1$$
$$z_{j-1} \leftarrow z_{j-1} - 1$$

Else:

Go to the next loop

Repeat **3** until $z_i \leq z_i^{th}$ for all sites.

4. Return to **2**.

2.2 Validation

If the mechanism of the Oslo model is implemented correctly, for $L = 3$ and $p = 1$, the time evolution of the system must follow the process in Fig 2. and the series of avalanche sizes s must be $\{0, 1, 0, 2, 1, 0, 3, 3, 3, ...\}$, where the leading 0 is the size of the avalanche triggered by the addition of the first grain.

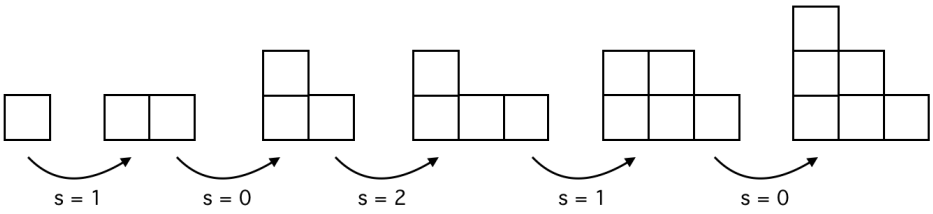

Figure 2: Time evolution of an Oslo model with $L = 3$. The threshold slope at each site is fixed to be 1. The size of each avalanche triggered between two stable states is indicated in the plot. The configuration will not change after the above iterations and the avalanche sizes thereafter are always 3.

Let $L = 3$ and $p = 1$, the program returns the expected avalanche-size series. The time series of the system height is $\{1, 1, 2, 2, 2, 3, 3, 3, 3...\}$, which is also evident in Fig 2.

Set $p = 0.5$ and measure the average heights $\langle H(L) \rangle$ of systems with various sizes in the steady state, in which $\langle$no. of grains added$\rangle$ = $\langle$no. of grains leaving$\rangle$, it turns out $\langle H(16) \rangle \approx 26.5$ and $\langle H(32) \rangle \approx 53.9$, suggesting that in the steady state, instead of appearing with equal probability, z_i are more likely to be 2. This phenomenon can be understood through a thought experiment.

Consider all possible forms of slope as illustrated in Fig 3. and initialise a system in which the quantity ratio of different slope types I:II:III:IV:V is $\frac{1}{4} : \frac{1}{4} : \frac{1}{6} : \frac{1}{6} : \frac{1}{6}$ (because $p = P(\mathrm{I}) + P(\mathrm{II}) = P(\mathrm{III}) + P(\mathrm{IV}) + P(\mathrm{V}) = 0.5$). When one grain is added to the system, the sites with $z_i^{th} = 1$ have a higher probability to be relaxed than those with $z_i^{th} = 2$ because there are more II in the system than V. Therefore, the conversion of z_i^{th} from 1 to 2 occurs more frequently. Once the threshold slope of a site becomes 2, the slope at that site keeps growing as more grains are added until it reaches 2. Eventually, sites with $z_i = 2$ will become the majority.

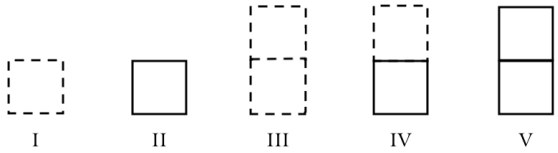

Figure 3: Possible forms of a slope at one site. The heights of the stacks represent the values of z_i^{th}, and the solid blocks are the actual grains in the pile. For example, Type IV shows that the threshold slope of a site is 2 and the site is able to hold one more grain.

Therefore, the algorithm behaves as expected and it can be used for further analysis.

3 The Height of the Pile

3.1 Time evolution of height

The time evolution of height in different systems are interpreted by the plot in Fig 4a. and the corresponding data collapse is shown in Fig 4b. Note that a unit time in the simulation is defined as the time separation between two consecutive additions of grain.

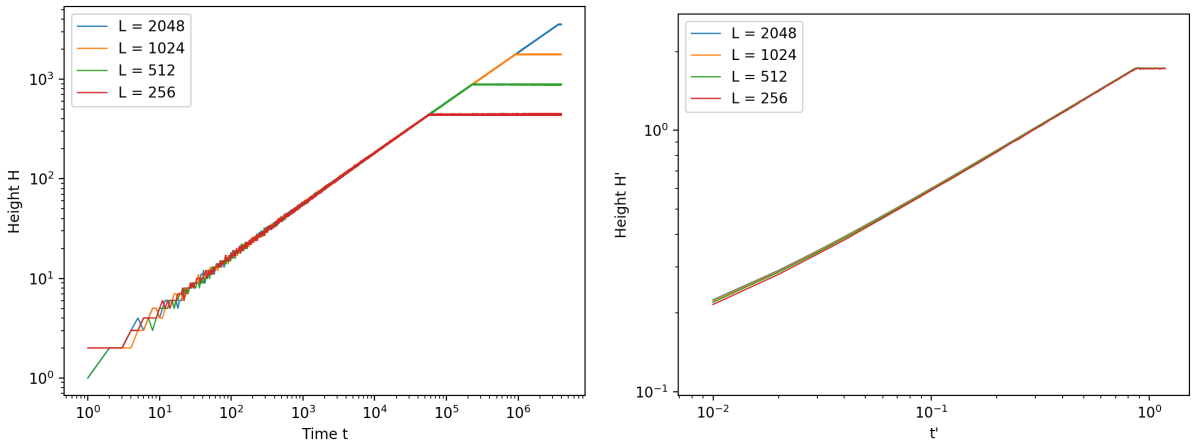

(a) Time evolution of height in systems of size $256, 512, 1024$ and 2048.

(b) Data collapse of height evolution.

Figure 4: The plots show clearly two distinct behaviours of height evolution; the height displays a power-law growth in the transient states, then oscillates about a constant when it reaches the set of recurrent states. The data collapse of the height evolution is shown in the right figure. The data overlap to a great extend.

It can be seen that the transition from transient states to the set of recurrent states occurs when the derivative of the plot in Fig 4a. is discontinuous (denote the cross-over time as $t_c(L)$). The height oscillates about a constant after $t_c(L)$ because the system keeps returning to states with $H(t, L)$ close to that constant if more grains are added. The steady state is the state in which $\langle$No. of grains added$\rangle$ = $\langle$No. of grains leaving$\rangle$, and it is equivalent to the set of recurrent states.

Before performing the data collapse shown in Fig 4b., two lemmas are proved as follows:

Lemma A:

In a 1D Oslo model with size L, the average height $\langle H_s(L)\rangle$ of the pile over time after reaching the steady state scales linearly with the system size.

Proof:

Assume that the largest possible threshold slope in a 1D Oslo model of size L is Z, where $Z \in \mathbb{Z}^+$, then the height of the system must not exceed ZL. In addition, once the system has reached the steady state, the average slope must be no less than 1, so the height must be at least L. Since the height in the steady state is bounded between L and ZL, its average is expected to scale linearly with L.

Lemma B:

In a 1D Oslo model with size L, the average time $\langle t_c(L)\rangle$ needed to evolve the system from the empty state to the steady state scales linearly with L^2.

Proof:

In the Oslo model, the time is measured by the number of grains that have been added to the system. Before $t_c(L)$, none of the grains leaves the system, so the time is equivalent to the number of grains remaining in the pile. When the system just reaches the steady state, the average slope must be between 1 and Z, where Z is the largest possible threshold slope. Therefore, the average quantity of grains $\langle N\rangle$ at $t_c(L)$ is bounded:

$$\sum_{i=1}^{L} i < \langle N\rangle < \sum_{i=1}^{L} Zi \tag{1}$$

$$\Rightarrow (L+1)L/2 < \langle N\rangle < (ZL+Z)L/2, \tag{2}$$

which suggests that $\langle t_c(L)\rangle$ is also bounded and scales with L^2.

Since $\langle H_s(L)\rangle = C_1 L$ and $\langle t_c(L)\rangle = C_2 L^2$, where C_1 and C_2 are coefficients of proportionality, they can be rearranged to be

$$\langle H_s(L)\rangle = C_1\sqrt{\frac{\langle t_c(L)\rangle}{C_2}}. \tag{3}$$

To produce a data collapse, a new coordinate system is introduced by eliminating the L

dependence:

$$t' = t/L^2 \tag{4}$$

$$H'(t') = \tilde{H}(t, L)/L, \tag{5}$$

where $\tilde{H}(t, L)$ is the average of $H(t, L)$ obtained from multiple simulations. The equation for the data collapse is

$$H'(t') = C_1\sqrt{\frac{t'}{C_2}}, \tag{6}$$

and the corresponding plot is in Fig 4b.

Since the height is proportional to $\sqrt{t}$ during transient states and behaves as a constant in the steady state, a modifying function $\mathcal{F}(x)$ is required. The complete equation is proposed to be:

$$\tilde{H}(t, L) = C_1 L \cdot \mathcal{F}\Big(\frac{t}{\langle t_c(L)\rangle}\Big), \tag{7}$$

where

$$\mathcal{F}(x) = \begin{cases} \sqrt{x}, & \text{for } x \ll 1 \\ 1, & \text{for } x \gg 1. \end{cases} \tag{8}$$

By substituting t with $t'L^2$ and $\tilde{H}(t, L)$ with $H'(t')L$ in Eqn 7, it becomes clear that the coordinate at the cross-over time in Fig 4b. is (C_2, C_1).

3.2 Estimation of the averaged cross-over time

The cross-over time $t_c(L)$ is equivalent to the number of grains in the system at $t_c(L)$ as proved in the proof of **Lemma B**, so it is convenient to count the number of grains instead to measure $t_c(L)$. Assume that z_i are equal to the average of the slopes $\langle z\rangle$, the heights at different sites form an arithmetic series in which $h_i - h_{i+1} = \langle z\rangle$. The sum of the series is

$$\begin{aligned} \langle t_c(L)\rangle' &= N \\ &= \sum_{i=1}^{L} \langle z\rangle i \\ &= \frac{\langle z\rangle}{2} L^2(1 + \frac{1}{L}) \\ &= \frac{\langle H_s(L)\rangle}{2}(L + 1), \end{aligned} \tag{9}$$

where $\langle H_s(L)\rangle = \langle z\rangle L$.

The data of $\langle t_c(L)\rangle$ and $\langle H_s(L)\rangle$ were obtained by running 500 simulations for a certain system and taking the averages of $t_c(L)$ and the heights at $t_c(L)$. Then, $\langle t_c(L)\rangle'$ was estimated using Eqn 9.

The plot of the simulation result and predicted values is shown in Fig 5a and the error plot is in Fig 5b. The error scales with $L^{-0.849}$, so it vanishes as $L \to \infty$, which suggests that the prediction is correct.

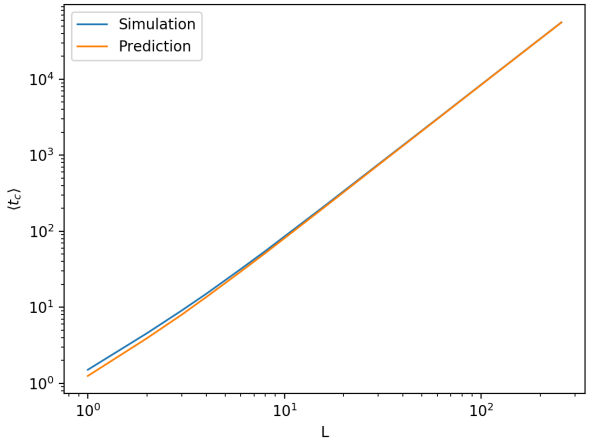

(a) Simulation data and prediction of $\langle t_c(L) \rangle$.

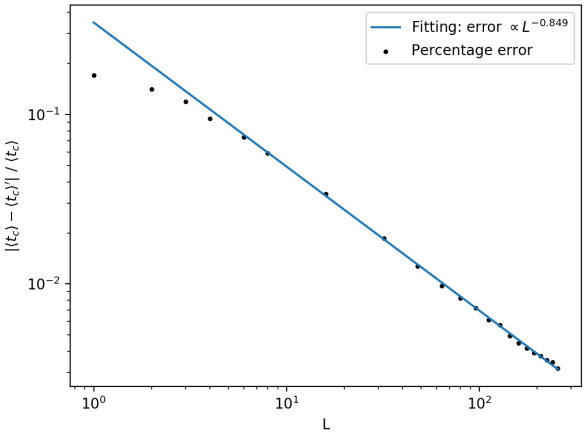

(b) Percentage error of predicted values of $\langle t_c(L) \rangle$.

Figure 5: (a) shows that the simulation result is very close to the predicted values. (b) shows that the percentage error of the prediction is proportional to $L^{-0.849}$.

3.3 Scaling of the average height after the cross-over time

As mentioned earlier, $\langle H_s(L) \rangle$ is the average height of a system of size L after $t_c(L)$. It is estimated and plotted against different L in Fig 6a.

A linear function seems to fit the data in Fig 6a. very well, but the residual plot in Fig 6b. shows a non-linear pattern, so there must be some other higher-order terms that present in the relation between $\langle H_s(L) \rangle$ and L.

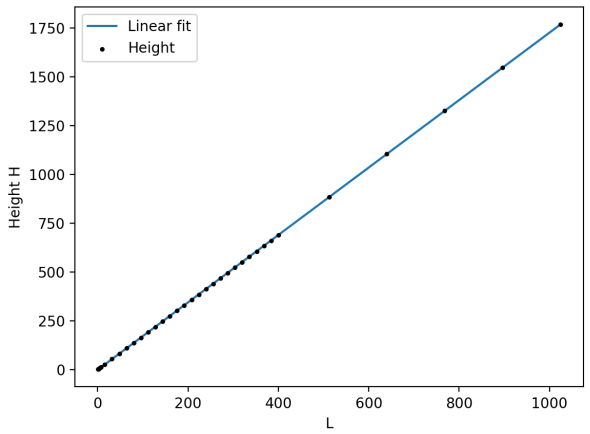

(a) $\langle H_s(L) \rangle$ v.s. L.

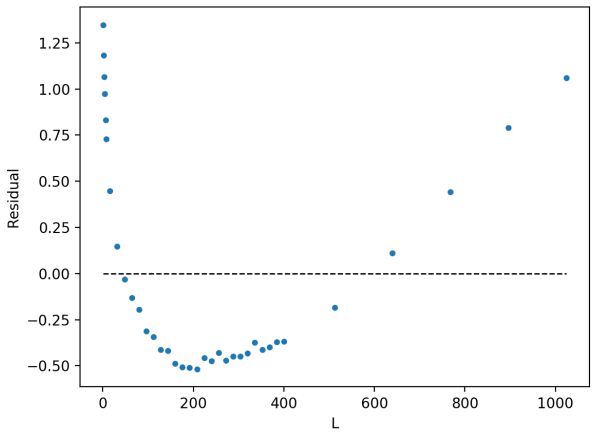

(b) Residual plot of the fitting in Fig 6a.

Figure 6: (a) shows that $\langle H_s(L) \rangle$ almost scales linearly with L, which confirms **Lemma A** in Section 3.1. The coefficient of proportionality is around 1.729. (b) is the residual plot of the former and its non-linear pattern suggests that there exist corrections to scaling.

Assume that $\langle H_s(L) \rangle = a_0 L(1 - a_1 L^{-\omega_1} + a_2 L^{-\omega_2} + ...)$, where a_i are constants and $\omega_i > 0$. The values of a_0 and ω_1 are of particular interest and can be estimated by neglecting terms whose orders are higher than ω_1. The equation can be alternatively expressed to produce a linear relation:

$$\ln\left(1 - \frac{\langle H_s(L) \rangle}{a_0 L} + O(\omega_2)\right) = -\omega_1 \ln L + \ln a_1 \tag{10}$$

The value of a_0 is carefully tuned so that the plot of Eqn 10. behaves linearly when L is large (shown in Fig 7.) because terms with higher orders vanish as $L \to \infty$.

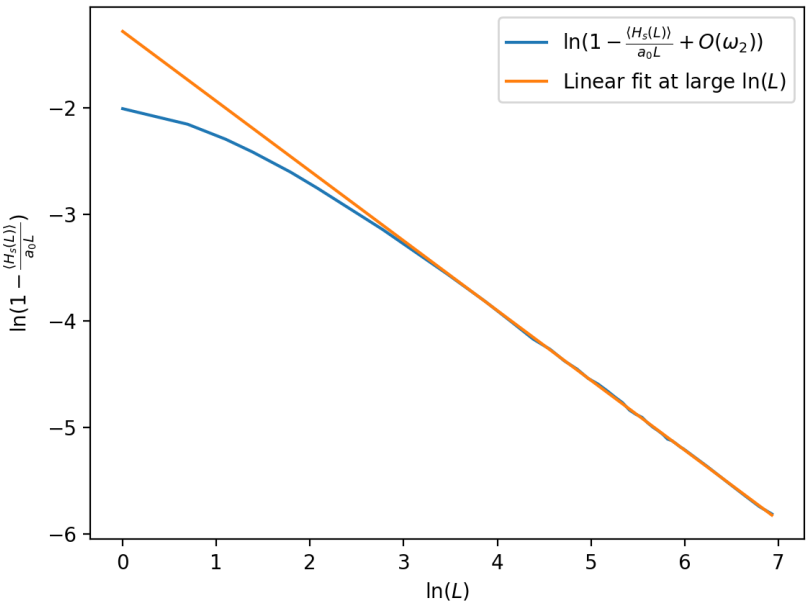

Figure 7: The plot of Eqn 10. and its linear fitting. The value of a_0 is 1.7333 ± 0.0001 when the linear function best fits the data at large L (coefficient of determination ≈ 0.9997). The value of the slope ω_1 is -0.655 ∓ 0.005.

As a result, the estimated value of a_0 is 1.7333 ± 0.0001 and the corresponding ω_1 is 0.655 ∓ 0.005.

3.4 Scaling of standard deviations of height & slope

The standard deviation of the height σ_H after $t_c(L)$ is

$$\begin{aligned} \sigma_H(L) &= \sqrt{\langle H_s^2(t,L)\rangle - \langle H_s(t,L)\rangle^2} \\ &= \sqrt{\lim_{T\to\infty} \frac{1}{T} \sum_{t=t_0+1}^{t_0+T} H_s^2(t,L) - \left[\lim_{T\to\infty} \frac{1}{T} \sum_{t=t_0+1}^{t_0+T} H_s(t,L)\right]^2}, \end{aligned} \tag{11}$$

where $t_0 > t_c(L)$ [2].

The value of $\sigma_H(L)$ is calculated and plotted in Fig 8a. The standard deviation of the slope $\sigma_z(L)$, defined as $\sigma_H(L)/L$, is also plotted against L in Fig 8b.

In Fig 8a. and 8b., $\sigma_H(L)$ scales with $L^{0.240}$, whereas $\sigma_z(L)$ decreases with $L^{-0.760}$. Therefore, $\sigma_z(L)$ approaches 0 and the averaged slope $\langle z\rangle$ converges to a constant as $L \to \infty$. Given that $a_0 \approx 1.733$ and $\sigma_z(1024) \approx 0.003$ (obtained from Fig 8b.), $[1.727, 1.739]$ is a 95% confidence interval for the value of $\langle z\rangle$ as $L \to \infty$.

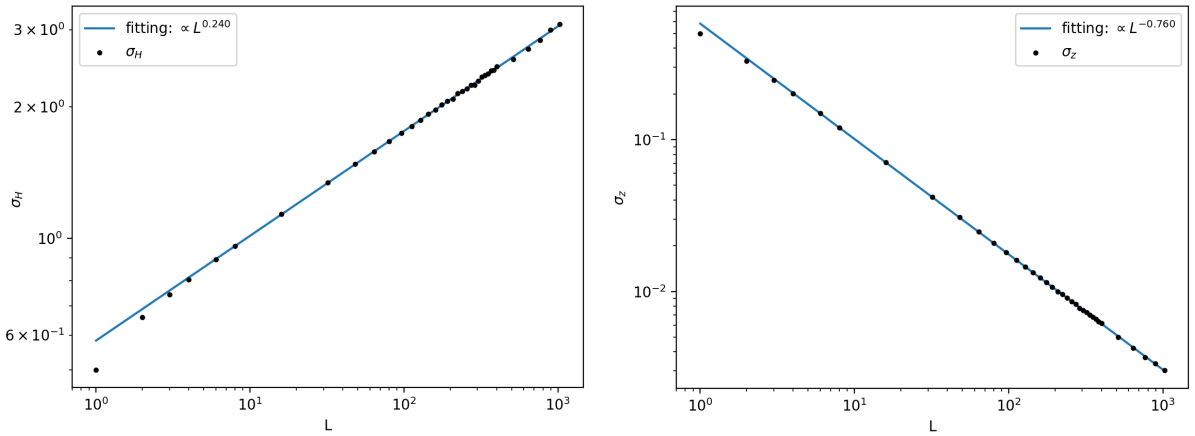

(a) $\sigma_H(L)$ v.s. L (b) $\sigma_z(L)$ v.s. L

Figure 8: The value of σ_H is proportional to $L^{0.240}$ and there is a sign of corrections to scaling at small L. $\sigma_z(L)$ scales with $L^{-0.760}$, which is expected because $\sigma_z(L) = \sigma_H(L)/L$. $\sigma_z(L)$ approaches 0 as $L \to \infty$.

3.5 Distribution of heights in the steady state

The probability of the occurrence of steady configurations with a certain height in a system of size L is defined as

$$P(H_s; L) = \frac{\text{No. of observed configurations with height H in a system of size L}}{\text{Total No. of observed configuration}} \text{[2]}. \quad (12)$$

Since $H_s = \sum_{i=1}^{L} z_i$, H_s is expected to be a discrete distribution that approximates a Gaussian distribution when $L \gg 1$ if z_i are independent and identically distributed (i.i.d.) variables with finite variance. The argument is based on the central limit theorem, which states that the sum of a large number of i.i.d. and finite variables tends towards a Gaussian distribution.

The height distributions of different systems are shown in Fig 9. Assume that they are all Gaussian distributions, the values of $\langle H_s(L) \rangle$ and $\sigma_H(L)$ obtained in earlier sections can be used to construct hypothesized Gaussian distributions for the actual data. The distributions are constructed through

$$P(H_s; L) = \frac{1}{\sqrt{2\pi}\sigma_H(L)} \exp\Big(-\frac{(H_s - \langle H_s(L) \rangle)^2}{2\sigma_H^2(L)}\Big), \quad (13)$$

which are also shown in Fig 9 and seem to agree with the simulation results.

To get a better visualisation, a data collapse is performed on the simulation data (assume they are Gaussian distributed). Eqn 13. is rearranged to be

$$P(X)\sigma_H(L) = \frac{1}{\sqrt{2\pi}} \exp\Big(-\frac{X^2}{2}\Big), \quad (14)$$

where

$$X = \frac{H_s - \langle H_s(L) \rangle}{\sigma_H(L)}. \quad (15)$$

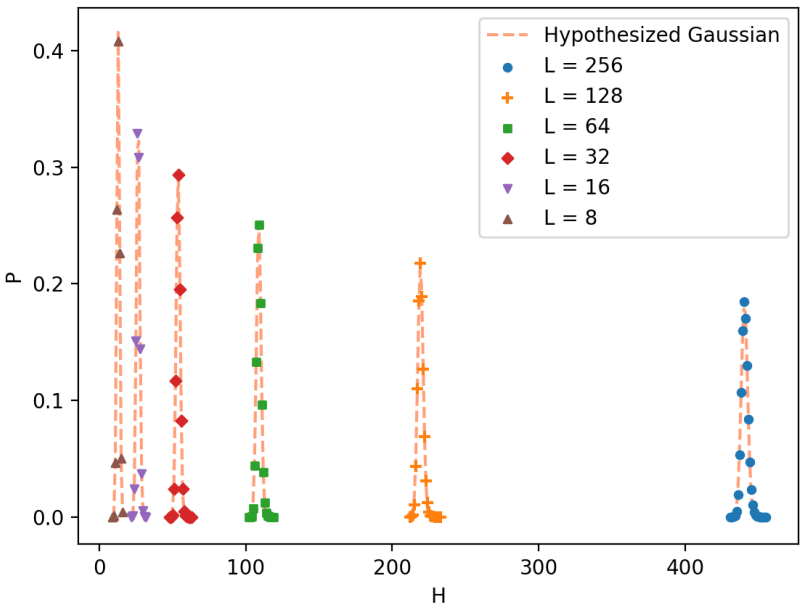

Figure 9: Height distributions of systems with different sizes and their hypothesized Gaussian distributions. The Gaussian distributions seem to agree with the actual data at a large scale.

The data collapse is shown in both Fig 10a. and 10b. with two different scalings. The actual distribution in Fig 10a. is skewed slightly to the left. Since the logarithm of a Gaussian distribution preserves the symmetry identity, the plot in Fig 10b. gives a better presentation of the skewness of the height distribution.

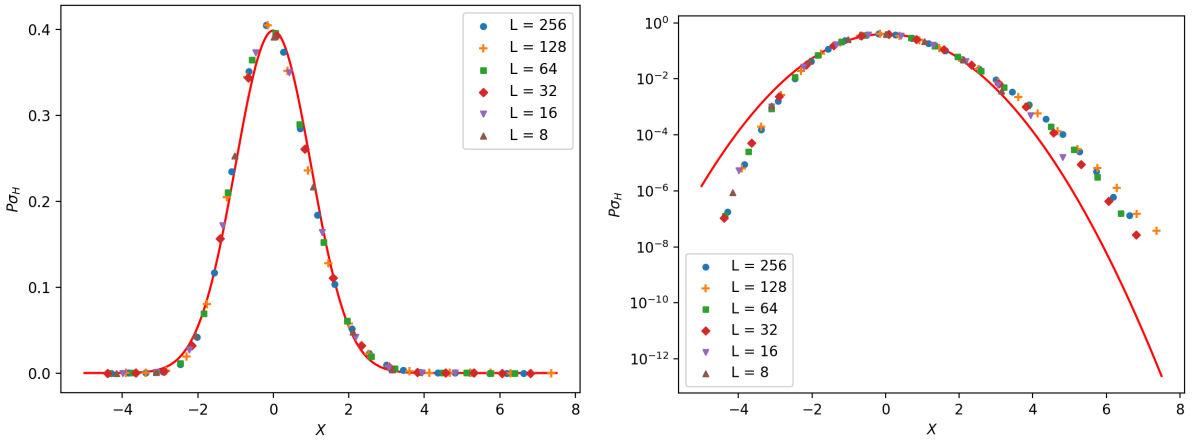

(a) Data collapse of height distributions.

(b) Log-linear plot of the data collapse

Figure 10: Two plots show the data collapse of height distributions of different systems. The red line is the idealised Gaussian distribution centered at 0 with $\sigma = 1$. The log-linear plot in (b) magnifies the asymmetry presented in the actual distribution.

It is expected that the distribution is skewed to the left: the height of a system has a higher probability to reach H_s^i than H_s^j, where $H_s^j > H_s^i > \langle H_s \rangle$, from lower values; however, if the height is H_s^j, the system has the potential to lose more height through an avalanche than if the height is H_s^i. Therefore, the height distribution appears to be skewed to lower values.

If z_i are truly i.i.d. variables, $\sigma_H(L)$ would have scaled differently. Since z_i can only be 1 or 2 (neglect $z_i = 0$ as the probability is small), the value of each z_i can be reduced by 1 to make a binomial distribution, and the probability of $z_i = 0$ (after reduction) is p. The reduction only affects the mean of the height but does not change $\sigma_H(L)$ of the distribution. Then, the height distribution becomes a binomial distribution with L trials, so $\sigma_H(L)$ is equal to $\sqrt{Lp(1-p)}$. The value of $\sigma_H(L)$ scales with $\sqrt{L}$, which grows much faster than $L^{0.240}$ as shown in Fig 8a.

The reason that the actual height distribution has smaller $\sigma_H(L)$ because z_i are, in fact, not i.i.d. variables; each z_i depends on z_j for all $j < i$. Most of the time when a grain is added to the system, z_i are not changed at sites with large i because the avalanche size is small. As a result, the variance of the height is greatly reduced.

4 Analysis of Avalanches in Different System

4.1 The avalanche-size probability

The size of an avalanche s is defined as the number of topplings in one iteration (one addition of a grain). The probability of a particular avalanche size is

$$P_N(s; L) = \frac{\text{No. of avalanches of size } s \text{ in a system of size } L}{\text{Total no. of avalanches } N}[2]. \tag{16}$$

The distribution of s in a system with $L = 256$ is plotted in Fig 11a. The data can be binned with bins that have a power-law growth. Each bin falls in an interval $[a^j, a^{j+1})$ for $j \in \mathbb{N}$ and a is a constant so that the bin widths appear to be constant in the log-scaled axis. Note that $s = 0$ cannot be log-binned because 0 cannot be represented in a log-scaled axis. Fig 11b. is an example of a log-binned distribution.

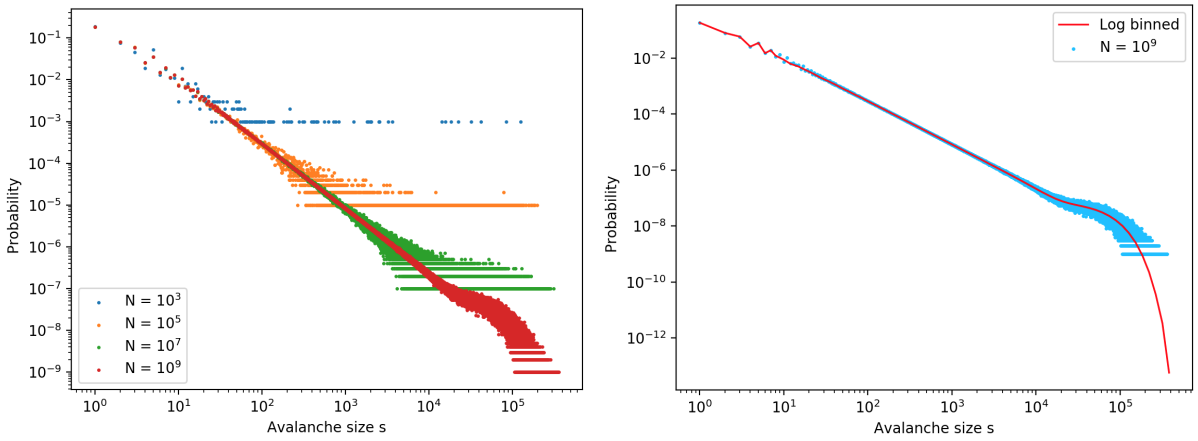

(a) Convergence of avalanche size distribution in a system with $L = 256$.

(b) Log-binned distribution of samples of size 10^9

Figure 11: (a) shows the distribution of different sample sizes in a system of size 256. The distribution converges as more avalanches are measured. (b) gives a comparison of the discrete distribution and its log-binned version. The parameter a of of the bin width is 1.2.

Fig 11b. shows that the distribution rises slightly (forming a characteristic "bump") and then falls rapidly at large s. This phenomenon can be explained as follows.

Imagine a finite system Ω_L of size L is the top part of an infinite system Ω_∞ (Ω_L is a subset of Ω_∞), and the largest possible avalanche size in Ω_L is S. In one iteration, Ω_L triggers a sufficiently large avalanche of size s_i, which causes some grains to leave the system. However, the leaving grains are still in Ω_∞ and they keep toppling outside Ω_L. Assume the avalanche size in Ω_∞ is s_j such that $s_j > S$. In the next iteration, the avalanche size is s_i in both Ω_L and Ω_∞, which means no further topplings outside Ω_L.

In the above example, the probability of $s = s_i$ in Ω_L is the sum of the probabilities of $s = s_i$ and $s = s_j$ in Ω_∞. It can be inferred that the probability of any avalanche size larger than S is re-distributed to smaller ones in Ω_L. As a result, the probability distribution in Ω_L rises at large s. In addition, the probability must decrease to 0 beyond the maximum avalanche size S, so it falls dramatically in the tail. The rapid decay also offsets the probability increase at smaller s such that the distribution is normalised.

The log-binned plot for different systems is shown in Fig 12a. The distributions are overlapped on a straight line at $s > 10$ except for the "bumps", which suggests that the distribution follows a power-law decay as $L \to \infty$. Therefore, the log-binned probability $\tilde{P}(s; L)$ should follow a finite-size scaling (FSS) ansatz:

$$\tilde{P}(s; L) = c_1 s^{-\tau_s} \mathcal{G}(s/s_c) \text{ for } s \gg 1, L \gg 1 \text{ [3]}, \tag{17}$$

where $s_c = c_2 L^D$ (because the "bumps" seem to be evenly spaced in the log-log plot), c_i are constants and $\mathcal{G}(s/s_c)$ a function that adjusts the behaviour of the distribution beyond s_c (the "bump") and has the form:

$$\mathcal{G}(x) \propto \begin{cases} \mathcal{G}(0) + \mathcal{G}'(0)x + \frac{1}{2}\mathcal{G}''(0)x^2 + \ldots & \text{for } x \ll 1 \\ \text{decay rapidly} & \text{for } x \gg 1. \end{cases} \tag{18}$$

The data collapse can be performed by putting $s^{\tau_s}\tilde{P}(s; L)$ in the $y-$axis, which aligns the power-law decay part horizontally, and s/L^D in the $x-$axis, which overlaps the "bumps". The data collapse is shown in Fig 12b.

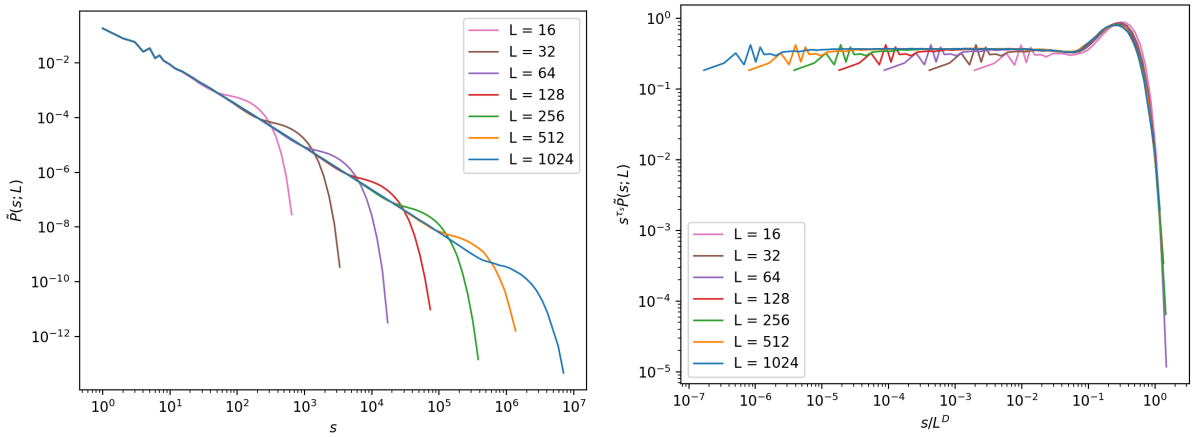

(a) Log-binned avalanche-size distribution of systems of different sizes.

(b) Data collapse of avalanche-size distributions

Figure 12: (a) is the log-binned plots for different systems. 10^8 avalanches are measured in each system and the binning parameter a is 1.2. (b) is the data collapse of the former plot. The values of τ_s and D are 1.551 ± 0.005 and 2.250 ± 0.005 respectively.

While doing the data collapse, only systems of size $256, 512, 1024$ are considered in the process of alignment because of corrections to scaling. The values of τ_s and D are carefully tuned, which turn out to be 1.551 ± 0.005 and 2.250 ± 0.005 respectively.

4.2 The moment of avalanches

The $k-$th moment of avalanches $\langle s^k \rangle$ in a system of size L is defined to be

$$\langle s^k \rangle = \lim_{N \to \infty} \sum_{s=1}^{\infty} s^k P_N(s; L), \tag{19}$$

where s are measured at time $t > t_c(L)$. Replace $P_N(s; L)$ with $\tilde{P}(s; L)$ and summation with integration, Eqn 19. can be expressed as a proportion relation:

$$\begin{aligned} \langle s^k \rangle &\propto \int_1^{\infty} s^{k-\tau_s} \mathcal{G}\Big(\frac{s}{c_2 L^D}\Big) ds \\ &\propto L^{D(1+k-\tau_s)}, \end{aligned} \tag{20}$$

in which the integration is done through variable transformation. Therefore, $\langle s^k \rangle$ v.s. L is expected to be a straight line on the log-log plot. The measured data (obtained from 10^8 avalanches per system) are plotted in Fig 13a. and the corrections to scaling are shown in Fig 13b.

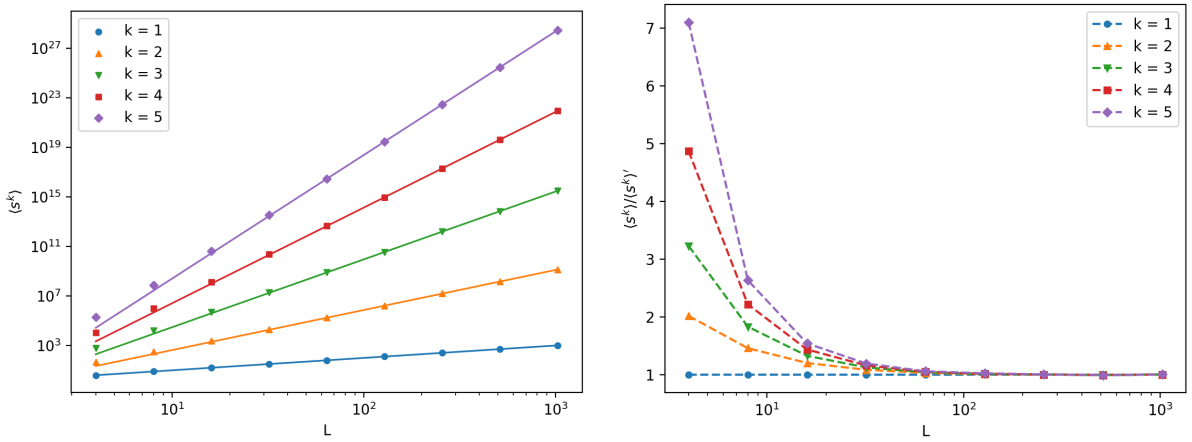

(a) $\langle s^k \rangle$ v.s. L for various k and their fitting functions.

(b) Corrections to scaling of $\langle s^k \rangle$.

Figure 13: The values of $\langle s^k \rangle$ for each k seem to follow a power-law growth with corrections to scaling. The data at $L > 32$ in the left figure are fitted with functions $\propto L^b$, where $b = 1.00, 3.24, 5.48, 7.73, 9.98$ for $k = 1, 2, 3, 4, 5$ respectively. The plot on the right is obtained by plotting the quotients of the measured data and the points on the corresponding fitting function.

Fig 13a. and 13b. verify the previous prediction that $\langle s^k \rangle \propto L^b$ for some value of $b = D(1 + k - \tau_s)$ despite of corrections to scaling. Taking corrections to scaling into account, the difference between estimated values and measured data increases with k in a certain system, but the error drops rapidly as L becomes larger. Since the values of $D(1 + k - \tau_s)$ for different k are known, they are plotted against k to test whether it

grows linearly. The result is shown in Fig 14. and it clearly agrees with the theoretical prediction.

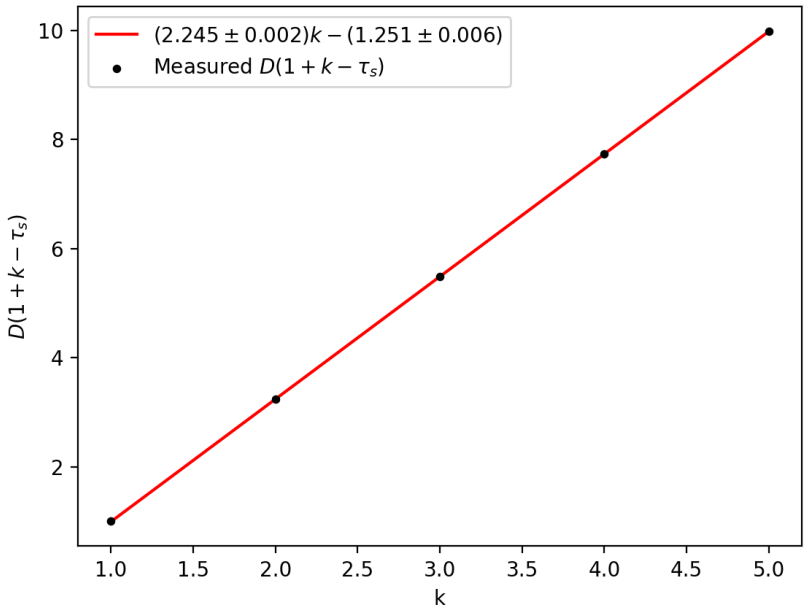

Figure 14: $D(1+k-\tau_s)$ v.s. k. The plot shows a linear trend with a slope D equal to 2.245 ± 0.002. The value of τ_s is 1.557 ± 0.003, which can be calculated from τ_s and the constant offset.

The values of τ_s and D are determined to be 1.557 ± 0.003 and 2.245 ± 0.002 respectively from the fitting parameters, which agree with the result obtained in Section 4.1.

5 Conclusion

The 1D Oslo model indeed displays scale invariance after it organises itself to the steady state. For a sufficiently large system at the steady state, the average height of the system should be equal to $(1.733 \pm 0.03)L$. The standard deviation of the coefficient will vanish as $L \to \infty$. The distribution of avalanche sizes also converges. As $L \to \infty$, the distribution tends to be a pure power-law decay that scales with $s^{(-1.557 \pm 0.003)}$. In a finite system, the power-law decay terminates at $s_c \propto L^{(2.245 \pm 0.002)}$ and it is followed by a "bump" and a rapid decay. The above relations should be applied to systems of large L because corrections to scaling bring significant errors if L is small.

References

[1] Bak, P., Tang, C. and Wiesenfeld, K. (1987). Self-organized criticality: An explanation of the 1/f noise. Physical Review Letters, 59(4), pp.381-384.

[2] Christensen, K. (2018). Complexity Project Notes. [online]. Centre for Complexity Science. Imperial College London [Accessed 10 Feb. 2019].

[3] FEDER, J. (1995). THE EVIDENCE FOR SELF-ORGANIZED CRITICALITY IN SANDPILE DYNAMICS. Fractals, 03(03), pp.431-443.